

# Kite performance testing by flying in a circle

**J. Stevenson**

Syft Ltd  
Christchurch, New Zealand

**K. Alexander**

University of Canterbury  
Christchurch, New Zealand

**P. Lynn**

Peter Lynn Kites  
Ashburton, New Zealand

## ABSTRACT

With the advent of recreational sports like kite surfing and buggying, the performance of kites has become a market driven item. Producers increasingly require methods to measure and improve the performance of the kites they manufacture. The Mechanical Engineering Department at the University of Canterbury has been working with a local kite producer to develop testing procedures suitable for kite manufacturers. The primary performance measurement is the lift to drag ratio. An early test rig was mounted in the top of a car, but limitations inherent in the design meant that it lost precision as the lift to drag ratio approached that of more advanced kites. This led the investigators to look for alternatives, and resulted in the development of the circular flight method. This method allows the test apparatus to be tuned to the performance of each kite, significantly improving the precision of the results while reducing the time taken for each test. In their raw form, the  $L/D$  results are not quite the same as those of the more traditional methods. But they reflect the underlying aerodynamic characteristics, and when used comparatively they can be used in the kite development process. Alternatively, with suitable processing the circular flight results can be converted to the traditional forms.

## NOMENCLATURE

$A_k$  kite area ( $m^2$ )  
 $C_D$  drag coefficient

$C_L$  lift coefficient  
 $D$  drag force (N)  
 $L$  lift force (N)  
 $L/D$  aerodynamic lift to drag ratio (weightless flight surface)  
 $L/D_t$  lift to drag ratio raw data from circular flight testing  
 $LTD$  kite lift to drag ratio (kite weight included)  
 $r$  'walking radius' or flier radius during circular testing (m)  
 $R$  radius of the flight circle (m)  
 $S$  line length (m)  
 $T$  line tension (N)  
 $V$  velocity or wind speed ( $ms^{-1}$ )  
 $\beta$  kite performance angle  
 $\lambda$  angle between  $r$  and  $S$   
 $\theta$  line angle relating to lift to drag ratio (LTD)  
 $\rho$  fluid density ( $kg/m^3$ )  
 $\psi$  angle between  $r$  and  $R$

## Subscripts

$g$  properties at the ground  
 $k$  properties at the kite  
 $w$  properties at the flyer (walking)  
 $\perp$  properties perpendicular to the line in circular testing

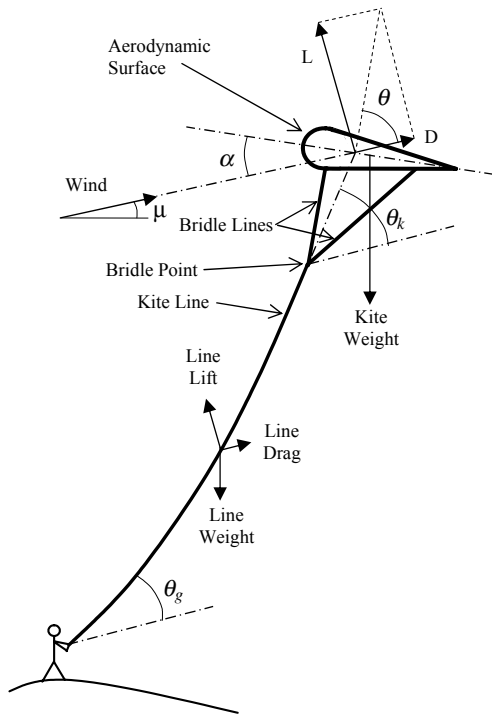


Figure 1. System diagram for a flying kite.

## 1.0 INTRODUCTION

The popularity of kite surfing and buggying has led to significant competition between kite manufacturers to produce high performance traction kites. To help the development process of a local kite producer Peter Lynn Kites Ltd, the Mechanical Engineering department at the University of Canterbury has been working on methods to test kite performance.

Although it is feasible to test kites in wind tunnels, traction kites either need very large wind tunnels or they need to be scaled down. Scaling has issues associated with the proper scaling of fabric properties and with line length. Traction kites are normally flown on lines approximately 30m in length, and on shorter lines new dynamic modes interfere with measurements. Given the small size of most kite manufacturing businesses, the cost of building or renting a large wind tunnel and the effort required to correctly scale down model kites is out of the question. The ideal is to test the actual kites at full scale.

The test methods developed through the University of Canterbury are intended to meet the needs of the kite industry without the requirement for wind tunnels. Low cost, quick set-up and the use of the full-sized kites are important features. Since kites can be built and modified quickly it is also necessary that the tests can be performed quickly, and that comparative results are available immediately.

The circular flight testing method described here goes a long way to meeting these requirements. The tests are quick, accurate and the apparatus can be adjusted for each kite. But the method requires a large building and the raw results are comparative only. This paper outlines the fundamental theory of circular flight testing, some of its characteristics, and the raw experimental results.

## 2.0 KITE AERODYNAMICS AND MEASUREMENTS

Figure 1 illustrates the key components of a kite. In essence a kite is a tethered wing with some sort of aerofoil section. In traditional kites this wing section is a single surface but the invention of ram air

structures has allowed other, more efficient, aerofoil shapes to be used. The wing is tethered to the ground using varying combinations of lines. Traction kites use two or more lines, which allow more control. Most modern traction kites have four lines as this provides the ability to change the angle-of-attack of the wing.

When a kite is flying in equilibrium the aerodynamic forces balance the gravitational forces and the line tension. When its angle-of-attack is changed the kite will move and rotate to redress that balance. The bridle point is where all the structural lines supporting the wing combine and connect to the main line or lines. This is a point about which the wing can be considered to rotate as it redresses imbalances. With four-line kites this point is located at the flyer on the ground.

The kite is subject to aerodynamic lift and drag which can be converted to lift and drag coefficients using the usual definitions:

$$C_L = \frac{L}{\frac{1}{2}\rho A_k V^2} \quad \dots (1)$$

and

$$C_D = \frac{D}{\frac{1}{2}\rho A_k V^2} \quad \dots (2)$$

Of all the determinants of kite performance the lift to drag ratio is the most important. In sailing applications the lift to drag ratio affects both the speed of the craft and the optimal sailing course. The larger the lift to drag ratio, the faster the craft will go and the closer to the wind it can sail. (For a more complete discussion of the relationship between high speed sailing and lift to drag ratio see Marchaj<sup>(1)</sup>)

There are a number of different lift to drag ratio definitions applicable to kites. The most common of these is shown in Fig. 1 and is defined as follows.

*L/D*: The lift to drag ratio of the kite aerodynamic surface alone. It is the lift to drag ratio that would be found if the kite was to be set up like a wing in a wind tunnel. The kite weight, line aerodynamics and line weight do not enter this definition, so that:

$$L/D = C_L/C_D \quad \dots (3)$$

The kite line angle or azimuth angle  $\theta$  for a weightless kite with no line interactions is therefore:

$$\theta = \text{Tan}^{-1}(L/D) \quad \dots (4)$$

*LTD<sub>k</sub>*: This is the lift to drag ratio at the kite, taking kite weight into account (but ignoring effects of the line). For the case where the relative wind is moving horizontally this is given by:

$$LTD_k = (L - m_k g) / D \quad \dots (5)$$

The kite line angle or azimuth angle  $\theta_k$  at the kite bridle point, for a kite where weight is included is therefore:

$$\theta_k = \text{Tan}^{-1}(LTD_k) \quad \dots (6)$$

Where the wind is at some angle  $\mu$  to the horizontal (as for example on the slope of a hill) then:

$$LTD_k = \frac{(L - m_k g \cos(\mu))}{(D + m_k g \sin(\mu))} \quad \dots (7)$$

*LTD<sub>g</sub>*: Finally there is the effective lift to drag ratio experienced by the operator on the ground. In the case of traction kiting, where the kite is used to sail a buggy or a surfboard, the *LTD<sub>g</sub>* is arguably the most important kite performance characteristic. That is because this definition takes into account all the forces acting on the whole kite system. So it gives the direction of the propulsion force used by the

flier. In this case the lift and drag of the kite line, as well as its weight are taken into account. A full analysis of the loads on the kite line has been undertaken by authors such as Goela *et al*<sup>(2)</sup>, and this was applied to traction kites by Stevenson<sup>(3)</sup>.

Associated with  $LTD_g$  when the line loads are included, is the azimuth angle at the ground  $\theta_g$ . This is defined as:

$$\theta_g = \text{Tan}^{-1}(LTD_g) \quad \dots (8)$$

### 3.0 PREVIOUS RESEARCH

In the past traction kite performance has been determined based on experience and approximate measurement methods. In contrast, the University of Canterbury project attempted to develop a kite testing procedure that delivered useful, repeatable results within known margins of error. The initial test rig developed for these measurements was mounted on the roof of a car and kites were flown above while driving along an empty beach<sup>(3,4)</sup>. Measurements of wind speed, line angle and line load, allowed  $LTD_g$  and  $C_{Lg}$  to be determined for each kite under different conditions. Vehicle-based test rigs of this type are not a new idea, an early example being the truck based parafoil test apparatus used by Nicolaidis and Tragarz<sup>(5)</sup>. However, it was felt that this rig, developed specifically for kites, would be of use to the company as it would not require a large capital outlay, and full-sized kites in a range of sizes could be tested quite quickly.

Although the rig was refined over a number of years there were inherent problems in the design that made it difficult to continue getting useful results. These problems stem from the tangent relationship between  $LTD_g$  and line angle (Equation (8) above) which meant that the accuracy of  $LTD_g$  was very sensitive to the accuracy of line angle measurements,  $\theta_g$ . Very small errors in the measured angle  $\theta_g$  resulted in large errors in the indicated  $LTD_g$ . For low performing kites the errors were acceptable. But the asymptotic nature of the tangent relationship meant that as kite performance got better the problem became worse. So as time went on and the kites improved, the method increasingly made itself obsolete.

The weather was also an issue with this method, as good tests could only be performed when natural wind speeds were very low. This limited the number of test days and often extended the time it took to obtain a complete set of results. Since kites can be constructed quickly, test results that took a long time to obtain were often out of date by the time they were taken. For testing to be useful to the company it was important to develop a quicker and more accurate test method.

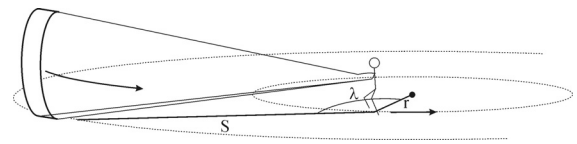


Figure 2. Flying a controllable kite in a circle showing the key measurements.

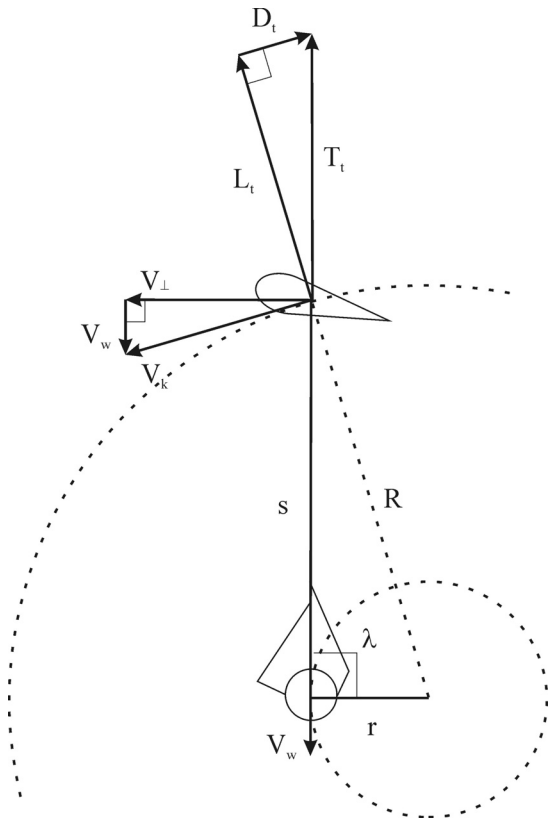


Figure 3. Plan view of a circular flight test with  $\lambda = 90^\circ$ .

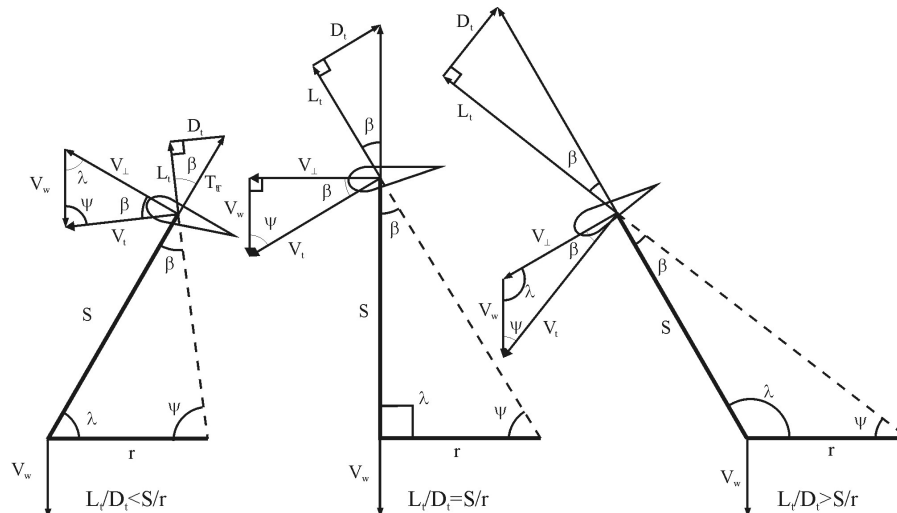
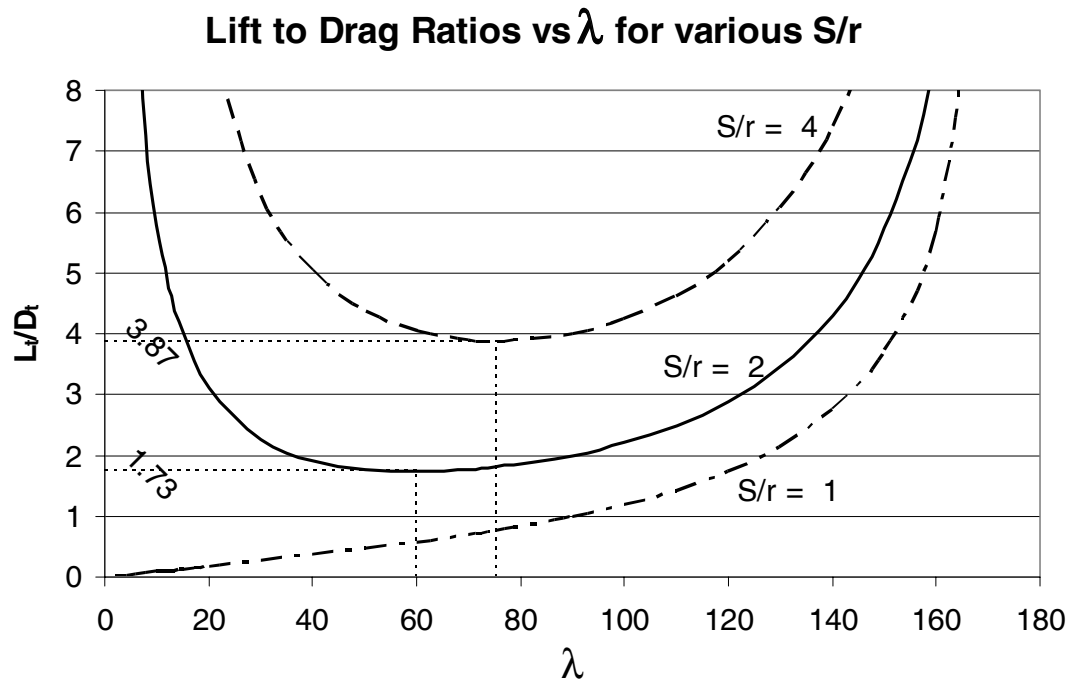


Figure 4. Generalised flying positions, relative to the walking circle radius.

Figure 5. Effect of varying  $S/r$  ratio.

## 4.0 CIRCULAR KITE TESTING

### 4.1 Outline of method

On a day when there is no wind it is possible to fly a controllable kite by walking backwards in a small circle and flying the kite in a larger horizontal circle. Figure 2 illustrates the method. Flying the kite in this manner allows the kite lift to drag ratio to be determined, as the lift to drag ratio is related to:

- The radius of the circle walked by the flyer,  $r$
- The length of the line attached to the kite  $S$ , and
- The angle  $\lambda$  between  $S$  and  $r$ .

To illustrate, assume that the flyer modifies the walking circle radius  $r$  until the kite is flying directly in front of him/her. In this case  $\lambda$  will be  $90^\circ$  as shown in the plan view of the system in Fig. 3. In this special case three similar triangles are formed. The first is formed by the physical arrangement of  $S$ ,  $r$  and an imaginary line between the centre of the circle and the kite,  $R$ . The velocity vectors at the kite form the second triangle. This is made up of the walking speed of the flyer  $V_w$ , the velocity of the kite perpendicular to the line  $V_{\perp}$ , and the tangential velocity of the kite  $V_k$ , which is also the apparent wind at the kite. From similar triangles the velocity of the kite perpendicular to the line  $V_{\perp}$  is given by:

$$V_{\perp} = \frac{S}{r} V_w \quad \dots (9)$$

The forces acting on the kite form the third triangle. The lift force  $L_t$  acts perpendicular to the direction of the apparent wind (that is, perpendicular to  $V_k$ ) while the drag force  $D_t$  acts parallel to  $V_k$ . Assuming an equilibrium condition has been reached the resultant force  $T_r$  must act along the kite line. (If the system is not in equilibrium the kite will accelerate or decelerate until the forces

balance). Since all these triangles are dimensionally similar the lift to drag ratio can be found by:

$$\frac{L_t}{D_t} = \frac{S}{r} \quad \dots (10)$$

The values of  $S$  and  $r$  can be found by the simple measurement of the line length and the radius of the circle walked. For a first approximation this is a disarmingly simple set of measurements to make to find the kite lift to drag ratio.

Moving away from this special case, if the dimensions  $r$  and  $S$  are fixed, then  $\lambda$  can be other than  $90^\circ$  and it will depend on the characteristics of the kite. There are three general positions that the kite can fly:  $\lambda$  equals  $90^\circ$ , as already described;  $\lambda$  greater than  $90^\circ$ , and  $\lambda$  less than  $90^\circ$ . Figure 4 illustrates these three positions showing the velocity vectors and force vectors as they apply in each case.

The force triangle is only similar to the velocity triangle and the physical setup when  $\lambda$  equals  $90^\circ$  so only in this case does Equation (10) apply. To determine the lift to drag ratio in the general case the angle  $\beta$  must be determined. The lift to drag ratio is related to  $\beta$  by the formula:

$$\frac{L_t}{D_t} = \frac{1}{\tan(\beta)} \quad \dots (11)$$

$\beta$  can be found by using the following equation:

$$\beta = \sin^{-1} \frac{r \sin(\lambda)}{\sqrt{r^2 + S^2 - 2rS \cos(\lambda)}} \quad \dots (12)$$

Therefore, to determine the lift to drag ratio of the kite the only parameters that are required are:

- the line length,
- the radius of the walking circle and
- the angle  $\lambda$  that the lines form with the radius of the walking circle.

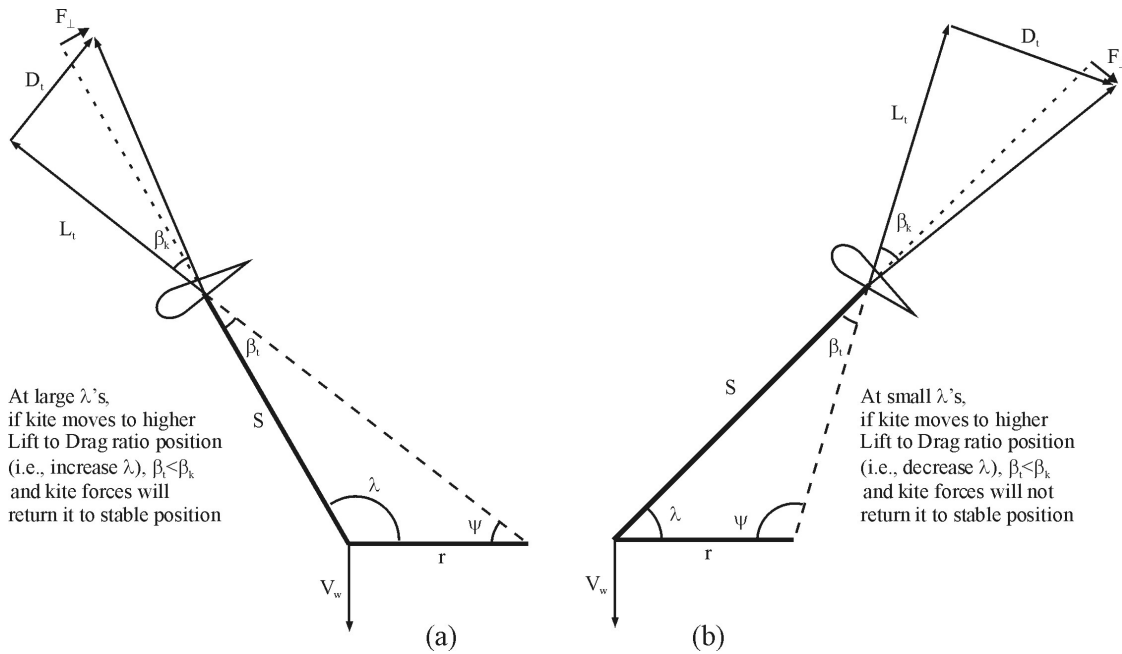


Figure 6. Restoring forces on a kite in a perturbed in flying location (shown).

**4.2 Circular flight compared to standard flight**

The lift to drag ratio obtained from circular testing is defined as  $L_t/D_t$ , to distinguish it from the usual definitions of the lift to drag ratio as defined in Equations (3), (5) and (7). In circular testing:

- The weight of the kite acts in a different plane to the lift and drag force;
- Centrifugal forces are present; and
- The kite line effects are different from those of a kite flown in a normal fashion.

While these effects are small they are not insignificant. They alter the loads so that the first approximation lift to drag ratio  $L_t/D_t$  in Equation (11) is not quite the same as the lift to drag ratio  $LTD_g$  of Equation (8). Techniques that allow for these load differences are quite involved, so for the purposes of this overview paper the differences are simply acknowledged, illustrated in Fig. 7, then put aside while the scope of the method is outlined.

**4.3 Varying rig dimensions**

By varying the line length  $S$  and the radius of the circle  $r$ , kites with different performance characteristics can be made to fly at different angles,  $\lambda$ . Figure 4 shows that  $\lambda$  is related to  $\beta$  by the equation:

$$\lambda = \pi - \beta - \text{Sin}^{-1}\left(\frac{S}{r} \text{Sin}(\beta)\right) \dots (13)$$

The relationship between the line angle  $\lambda$  and lift to drag ratio, for different  $S/r$  ratios, is shown in Fig. 5. This graph was constructed using Equation (13) and it indicates that if  $S > r$  (which is normally the case) there is a minimum ratio,  $L_t/D_t$  min, that a particular  $S > r$  can test. For example (see Fig. 5), for a setup of  $S > r = 2$ , the  $L_t/D_t$  min is approximately 1.73. It is not possible to fly a kite with a lower lift to drag ratio using an  $S > r = 2$ .

From Fig. 4 and Equation (11) it can be seen that the minimum lift to drag value is found when  $\beta$  is at a maximum. From Fig. 4 and using the sine rule

$$\text{Sin}(\beta) = \frac{r \text{Sin}(\psi)}{S} \dots (14)$$

where  $\psi$  is the angle between  $r$  and  $R$ . From Equation (14) the maximum value of  $\beta$  will occur when  $\psi$  equals  $90^\circ$  and the minimum lift to drag ratio that can be tested is

$$L_t / D_{tmin} = 1 / \text{Tan}(\text{Sin}^{-1}(r/S)) = \sqrt{S^2 - r^2} / r \dots (15)$$

Figure 5 indicates that above this minimum lift to drag ratio there are two possible angles  $\lambda$  where a kite with a given  $L_t/D_t$  can fly. In practical terms however, the kite will only sit at the larger of these two angles, as the lower angle is only neutrally stable and any perturbation will either cause it to go to the larger angle, or stop flying. This is illustrated in Fig. 6, which requires some explanation:

- Figure 6(a) and (b) both show the forces  $F$  on the system when the kite is perturbed from equilibrium to a line angle  $\lambda$  corresponding to a higher lift to drag ratio than the kite's actual lift to drag ratio (i.e.,  $\beta_k > \beta_i$ ).
- For  $\lambda$ s above  $L_t/D_{tmin}$ , (see Fig. 5) a larger lift to drag ratio corresponds to a  $\lambda$  larger than the stable value. In Fig. 6(a) the force  $F$  on the kite will return it to a stable position, decreasing  $\lambda$ .
- For  $\lambda$ s below  $L_t/D_{tmin}$ , (see Fig. 5) a larger lift to drag ratio corresponds to a smaller than the stable value. In Fig. 6(b), the force  $F$  on the kite will reduce  $F$  even further, rather than returning the kite to a stable flying location. So any perturbation will move the kite away from this stable point.

Thus Fig. 6 illustrates that the kite will only settle to the larger of the two  $\lambda$ 's representing its lift to drag ratio.

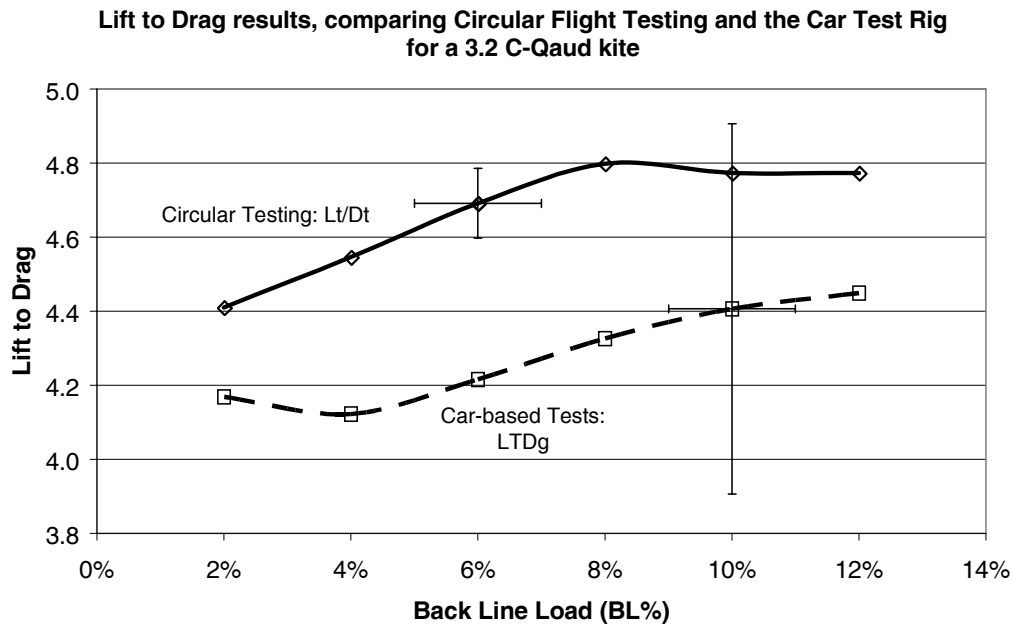


Figure 7. Comparative  $L/D$  results between circular testing and the car based test rig.

#### 4.4 Improved sensitivity by varying rig dimensions

As can be seen in Fig. 5, the lift to drag curves are relatively flat near the  $\lambda = 90^\circ$  point. If the line length  $S$  or the circle radius  $r$  is adjusted so that the kite is flying with  $\lambda \sim 90^\circ$  then  $L/D_t$  becomes insensitive to the accuracy of  $\lambda$ .

For example in Fig. 5, for  $S/r = 4$  any value of  $\lambda$  between about 70 and 83 degrees (that is  $\pm 6.5$  deg) gives a kite  $L/D_t$  of  $3.9 \pm 0.1$ . This is a good accuracy for a lift to drag ratio measurement. This is in contrast to the problems of the car roof method where, by Equation (8), to achieve the same  $\pm 0.1$  accuracy for  $LTD_g$  the angle  $\theta$  would have to be measured to  $\pm 0.3$  deg. It is very much easier to measure to an accuracy of  $\pm 5$  degrees than it is to measure to an accuracy of  $\pm 0.3$  degrees.

And when the kite performance is improved to an  $LTD_g$  of around 8, the requirement of the car roof method deteriorates even further to needing a precision of  $\pm 0.09$  degrees for the same accuracy of  $LTD_g$ .

Putting this the other way around, once the system is appropriately tuned, only a moderate precision in the measurement of  $\lambda$  is needed to measure  $L/D_t$  to a high accuracy. This means that with the relatively imprecise equipment that might be available to a kite manufacturer, the circular flight method can be used to resolve very small differences in  $L/D_t$ .

Being able to tune the test conditions for each kite in this way gives the circular testing method a significant advantage over other procedures.

#### 4.5 Bridle length

Prior to this point the line length  $S$  used in equations assumes that the kite does not have any bridles. However, the distance  $S$  is actually the distance to the lifting surface so the length of the bridle has to be included as part of the line length,  $S$ .

#### 4.6 Line tension and lift coefficient

If the line tension can be measured then a lift coefficient  $C_{L_t}$  can be determined also. The procedure is first to determine the kite lift  $L_t$  from:

$$L_t = \frac{T_t}{\sqrt{1 + \left(\frac{1}{L_t/D_t}\right)^2}} = T_t \cos(\beta) \quad \dots (16)$$

which can then be converted to a lift coefficient using Equation (1). (Note that the lift coefficient in this case is  $C_{L_t}$  which is slightly different from the  $C_L$  in Equation (1))

To find this coefficient the tangential velocity of the kite  $V_k$  needs to be determined by either:

- Measuring the time for one circuit, and calculating the circle size with the help of Equation (18) below; or by
- Measuring the velocity  $V_w$  at the flier and finding  $V_k$  from Equations (17), (18) below.

$$V_k = V_w \frac{R}{r} \quad \dots (17)$$

$$R = \sqrt{r^2 + S^2 - 2rS \cos(\lambda)} \quad \dots (18)$$

Equations (17), (18) are found from the geometry of the system as illustrated in Fig. 3. Thus the circular test method can be used to find a lift coefficient and by implication a drag coefficient as well.

#### 4.7 Results compared with standard kite measurements

To verify the theory behind circular flight testing, a purpose-built test rig was constructed and various kite tests performed. Figures 7 and 8 show comparisons between results obtained using the circular flight rig and the car-based rig. The kite used in these

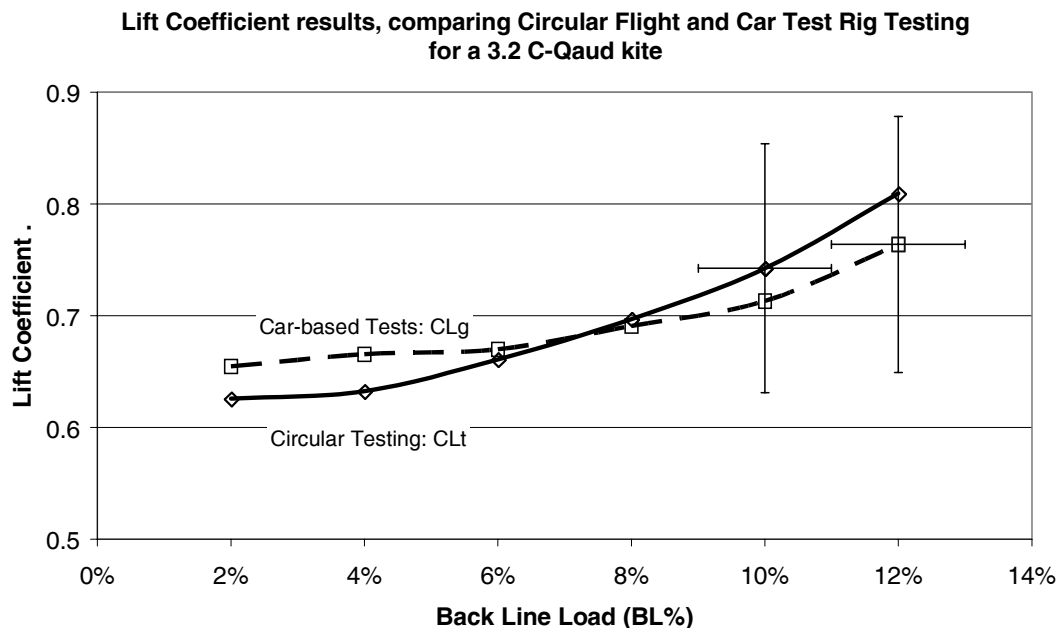


Figure 8. Comparative lift coefficient results between circular testing and the car based test rig.

tests was a four-line kite, the 3.2 C-Quad developed by Peter Lynn Kites. Although an old design, this particular kite was used extensively as the reference kite in the process of developing both test rigs. In both methods the kite was tested using 10m lines over a similar wind speed range. Performance figures for kites of this type are relatively immune to speed variation, so the results can be shown as a function of one variable, the back line load percentage (BL%). BL% is the proportion of the total line load taken by the aft control lines. Results shown in this way are relatively useful as BL% is one parameter that can be varied by the flyer to adjust kite performance.

Because there are different forces acting on the kite during circular testing as compared to the car rig tests, it is to be expected that the two methods should produce slightly different results. This is borne out in Fig. 7 which gives lift to drag results from the two methods for this reference kite. Figure 8, which gives lift coefficients, shows results which appear the same within experimental error.

In spite of the differences in lift to drag ratio (about 10%), the data from circular testing still reflect the underlying aerodynamics of the kite, so it is to be expected that both sets of data will show similar trends as the BL% is changed. This is apparent in both Figs 7 and 8.

Representative error bars are shown on Figs 7 and 8. For this particular kite the error in the lift to drag data was  $\pm 2\%$  for circular testing and  $\pm 10\%$  for the car-based test rig. This is indicative of the improved precision available from circular flight testing.

In Fig. 8 the lift coefficient data shows an error of approx  $\pm 15\%$  for both methods but for different reasons. The errors in the car-based test rig were caused by natural wind, load measurement errors, wind speed measurement errors, and angle measurement errors; all contributing. With the circular test method however, the error was caused primarily by one inferior instrument. With reasonable instrumentation the error in the lift coefficient using circular testing should easily be reduced to  $\pm 5\%$ .

## 5.0 USING THE DATA FROM CIRCULAR FLIGHT TESTS

Results from the circular flight method do not compare directly with the results from other methods as shown in Fig. 7, and these differences result from points noted in 4.2 above. To make a direct comparison however, techniques have been developed to convert the circular flight data on to the same basis as the traditional performance measurement in Equation (3). While these conversion techniques are relatively simple to apply, they are theoretically quite involved, and are not included here.

But from the kite development standpoint, this conversion is a step that need not be taken. Given that circular flight testing reflects the underlying aerodynamic performance, it is perfectly usable in its present form. Comparative tests can be undertaken to see whether the  $L/D_i$  has improved with a particular kite modification or not. And this is often all that is required. So the method, as it stands, can be used for kite development work, without ever needing to translate the results into the more conventional form.

## 6.0 CONCLUSION

Circular flight testing has advantages over other kite test methods in that it is quick, and the testing apparatus can easily be tuned to suit each kite. This tuning is especially advantageous as it allows the measurement sensitivity to be enhanced in the area of interest. Although the results in their raw form are not identical to traditional measurements of kite performance, techniques exist to convert from one to another. But even without this conversion, measurements using circular flight do reflect the underlying aerodynamics, so they can be employed for kite development even in their raw form, by the use of comparative test techniques.

## REFERENCES

1. MARCHAJ, C.A. *Aero-hydrodynamics of Sailing*, Dodd, Mead and Company, 1979, NY.
2. GEOLA, J.S., SOMU, N., ABEDINZADEH, R. and VIJAYKUMAR, R. Wind loading effects on a catenary, *J Wind Eng and Ind Aerodynamics*, 1985, **21**, pp 235-249.
3. STEVENSON, J.C. Traction Kite Testing and Aerodynamics, 2003, University of Canterbury. (Thesis:PhD), 2003.
4. ALEXANDER K.V. & STEVENSON J.A Test rig for kite performance measurement. *Proc Instn Mech Engrs*, v215, Part B, 2001, pp 595-598.
5. NICOLAIDES, J.D. and TRAGARTZ, M.A. Parafoil flight performance. Technical report, June 1971, AFFDL-TR\_71-38, AD 731 143.